JOURNAL OF CATALYSIS 62, 253–263 (1980)

An Infrared Study of CO and NO Adsorption on Alumina-Supported Iridium Catalyst

F. SOLYMOSI AND J. RASKÓ

Reaction Kinetics Research Group, The University, Szeged, P.O. Box 105, Hungary

Received March 12, 1979; revised August 17, 1979

Infrared spectroscopic measurements were performed for NO and CO adsorbed on reduced and oxidized Ir supported on γ-Al_2O_3. Adsorption of NO on a reduced sample produced bands at 1900 and 1850 cm^{-1}. These bands are attributed to NO adsorbed as $NO^{+\delta}$ on metal atoms of larger iridium crystallites (Site A) and on iridium atoms influenced strongly by the support (Site B), respectively. Spectra of NO adsorbed on an oxidized sample showed only a single band at 1950 cm^{-1}. This band is assigned as $NO^{+\delta}$ on partially oxidized Ir sites. CO adsorption on a reduced sample produced bands at 2070–2060 and 2020 cm^{-1}, which are associated with CO linearly bonded to Site A and Site B, respectively. Oxidation of the sample and subsequent adsorption of CO caused a band only at 2060 cm^{-1}, which is assigned as CO linearly bonded to Site A. Detailed investigations were made on the effect of the pressure, adsorption temperature, and evacuation at different temperatures on the intensities of the above bands.

INTRODUCTION

A great effort is currently being made to understand the surface interaction of NO and CO on noble metals, mainly because of its bearing on the performance of noble metals as catalysts for the reduction of NO pollutant. Much new information has been obtained with single crystals via the different modern surface techniques. In the case of dispersed metal, however, transmission infrared spectroscopy still represents one of the best and simplest tools to study the structure of chemisorbed species.

Recently, great attention has been paid to the chemisorption of the above gases on supported rhodium catalyst. It was first claimed by Garland *et al.* that at low rhodium concentrations the metal approached atomic dispersion (*1, 2*). It was further assumed that at 0.9 wt% Rh on γ-Al_2O_3 Rh exists as isolated atoms (*3*). Possibly as a result of the high dispersion, it was observed by different research workers that two CO molecules adsorb on one Rh atom, yielding the surface species 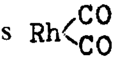 $\mathrm{Rh}\genfrac{}{}{0pt}{}{\diagup \mathrm{CO}}{\diagdown \mathrm{CO}}$ (*1–6*). The existence of this surface species was confirmed in experiments involving isotopically labeled gases, and it was also shown that there is an angle of ~90° between the CO groups (*6*).

Based on the appearance of a new doublet in the infrared spectrum during the coadsorption of NO + CO on supported Rh, the formation of 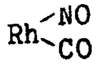 $\mathrm{Rh}\genfrac{}{}{0pt}{}{\diagup \mathrm{NO}}{\diagdown \mathrm{CO}}$ was postulated, which seemed to play an important role in the formation of isocyanate species on Rh at low temperature (*4, 5*).

In the present work, which is a continuation of studies carried out in this laboratory on the chemisorption of NO and CO and their surface interaction on metal oxides and supported nobel metals, we report on the adsorption of NO and CO on Ir/Al_2O_3 catalyst. In our next paper we shall give an account of the formation and stability of isocyanate species formed in the NO + CO reaction on this catalyst.

As concerns iridium catalysts, only a few infrared studies have previously been reported on the adsorption of CO. Lynds (*7*) noticed only one band at 2070 cm^{-1} for Ir

0021-9517/80/040253-11$02.00/0

supported on alumina. Guerra and Schulman (*8*) observed strong bands at 2030–2035 cm^{-1} and 2080 cm^{-1}, and weaker ones at 1993 and 1890–1910 cm^{-1} for Ir/SiO$_2$. Howe (*9*) found two bands, at 2060–2080 and 2020 cm^{-1}, for finely dispersed iridium supported by either alumina or silica, respectively.

No detailed infrared work has been published on the adsorption of NO on iridium. Only Unland (*10*), in a study of the formation of isocyanate complexes, reported a band at 1910 cm^{-1} for NO adsorbed on Ir/Al$_2$O$_3$.

EXPERIMENTAL

Materials. For the preparation of the supported iridium, 1 g $H_2IrCl_6 \cdot 6H_2O$ (Pierce Co.) was dissolved in 100 ml doubly distilled water. The calculated volume of the Ir-containing solution was added to an appropriate amount of support during constant stirring. The homogenized suspension was dried for 16 hr at 100°C, and then powdered in an agate mortar. The support used in this work was Al$_2$O$_3$ Degussa (P 110 Cl). The amount of Ir was 5 wt%.

Coherent, self-supporting tablets (30 × 10 mm) were prepared from 60 mg finely powdered material at high pressure. The sample thickness was estimated as 20 mg/cm^2. The disk was mounted in a quartz holder and was placed inside the infrared cell. Before adsorption and infrared spectroscopic measurements, the solid samples were treated in the infrared cell as follows: (i) evacuation for 90 min at 400°C; (ii) oxidation for 30 min with 100 Torr O$_2$ at 400°C; (iii) evacuation for 15 min at 400°C; (iv) reduction for 30 min with 100 Torr H$_2$ at 400°C; (v) evacuation for 15 min at 400°C.

Methods. Adsorption measurements were performed in a Sartorius microbalance. Infrared spectra were recorded at the temperature of the infrared beam (~50°C) with a Specord 71 ir double-beam spectrophotometer with an NaCl monochromator. The instrument scans the region from 4600 to 650 cm^{-1} at a rate of 1 or 5 wavenumbers/sec. The resolution was better than ±5 cm^{-1}. An attenuator was used in the reference beam to compensate the absorbance of the wafer itself. The instrument had facilities to expand the wavenumber scale fourfold and the absorbance scale 10-fold. All spectra were recorded as linear absorbance vs frequency.

The infrared experiments were performed in a Kiselev-type, greaseless infrared cell. Pretreatments of the tablets and high-temperature adsorption of gases were carried out in the upper part of the cell, around which a small furnace was placed. The temperature in this zone was measured with an Fe–Ko thermocouple inserted into glass thermowel. The lower part of the cell, which was situated in the infrared light, was sealed by NaCl windows with Torr-Seal low-vapor pressure resin. For the moving of the pellet from the upper part into the lower part of the cell, and vice versa, an electromagnet was used.

The cell was connected with a traditional evacuation and gas-handling system. This system is capable of attaining a vacuum of 10^{-5} Torr.

The dispersity of iridium was determined by adsorption measurements. The adsorptions of H$_2$, O$_2$, and CO have so far been used for this purpose (*11–17*). As regards the adsorption of H$_2$, the results agree that each iridium atom carries one hydrogen atom at monolayer coverage, whereas in the cases of CO and O$_2$ there is great controversy on the stoichiometries of adsorption. A difference in crystallite size seems to be the main cause of the divergences.

In the present work the dispersity of the reduced iridium sample was determined by H$_2$ titration, with the use of dynamic impulse method developed for the determination of the dispersity of platinum (*18*).

The results obtained are shown in Table 1. For comparison we also show the stoichiometry ratios of O/Ir and CO/Ir calculated from the adsorptions of O$_2$ and CO at 25°C.

TABLE 1

Characterization of Ir/Al_2O_3 Sample

	Number of experiments	H_2 adsorption at 25°C (μmole/g catalyst)	Dispersity (%)	Mean crystallite size[a] (Å)	Stochiometric ratio[b]	
					O/total Ir	CO/total Ir
Ir/Al_2O_3	1	84.9	65.2	15		
5 wt% Ir	2	81.2	62.4 64.1	16	0.59	0.30
	3	79.1	60.8 (average)	16		
	4	88.63	68.1	14		

[a] Calculated according to the equation derived by Corro and Gomez (*17*).

[b] Calculated from the value for the adsorption extrapolated to zero pressure at 25°C.

RESULTS

1. Adsorption Measurements

The adsorption of NO was investigated on a sample from the same batch used for infrared spectroscopic studies. Detailed adsorption measurements were carried out at 5 Torr at 25–150°C. The large volume of the balance chamber ensured a constant pressure to within 8–10% during the measurement. Some measurements were made at higher temperatures, too.

The adsorption of NO (5 Torr) on reduced surfaces started with a very fast initial uptake, followed by a very slow process (Fig. 1). The extent of initial gas uptake slightly increased with the temperature. Prolonged evacuation at 25°C resulted only in very small desorption even after adsorption at 25°C.

Mass-spectrometric analysis of the gas phase during adsorption revealed no products of the interaction between NO and the solid sample below 100°C. At 100°C a small amount of N_2O (0.16 μmole) was detected. Above 300°C the slow decomposition of NO began. The extent of NO decomposition on a freshly reduced sample at 300°C was ~10% in 1 hr. In the repeated experiment, without any pretreatment, the conversion of NO decreased.

The adsorption of NO was investigated

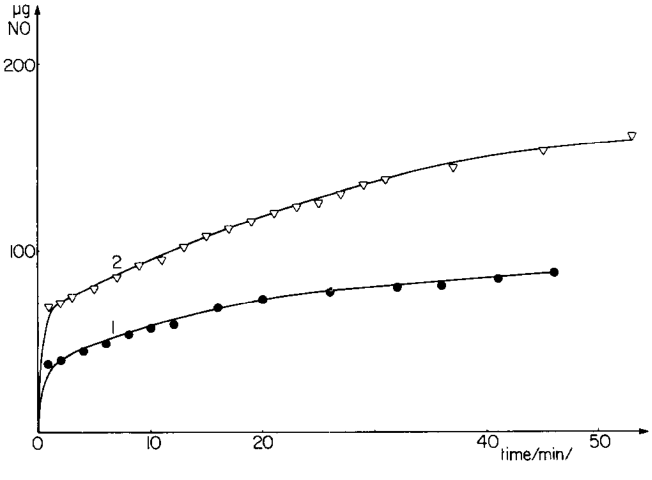

FIG. 1. Adsorption of NO (5 Torr) on reduced and oxidized sample at 25°C. (1) Oxidized surfaces; (2) reduced surfaces. The amount of the sample was 100 mg.

on oxidized surfaces. The sample was treated with 100 Torr O_2 at 400°C for 30 min, and the system then evacuated for 5 min and cooled down to the temperature of adsorption. On an oxidized surface the extent of initial uptake was less, and the entire adsorption was slower than on reduced surfaces. The adsorbed NO was strongly held on these surfaces, too.

In an attempt to calculate the approximate ratio between adsorbed NO and surface Ir atoms we determined the adsorption isotherm at 25°C. The amount of adsorbed NO at the saturation value on 1 g Ir/Al_2O_3 sample is 260 μmole. Taking into account the value for the adsorption extrapolated to zero pressure, we obtain a value of 0.62 for the NO/Ir ratio. This approaches the value for the O/Ir ratio determined by us.

The coadsorption of the NO + CO was studied at the same temperatures. For evaluation of the results, the adsorption of CO at a selected temperature was also examined. Some data are shown in Fig. 2. From a comparison of the three curves, it appears that the gas uptake from NO + CO mixture was only slightly less than the sum of the separately adsorbed gases.

2. *Infrared Spectroscopic Measurements*

a. NO adsorption. The adsorption of NO at room temperature on a *reduced surface* led to strong bands at 1900, 1850, and 1220 cm^{-1}, and weaker ones at 1950, 1620, 1590, 1560, and 1310 cm^{-1}. Some spectra are shown in Fig. 3.

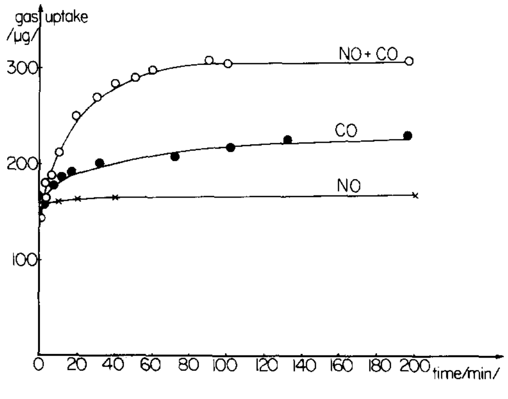

FIG. 2. Adsorption of NO (5 Torr), CO (10 Torr), and NO + CO gas mixture (15 Torr, mole ratio 1 : 2) on reduced sample at 300°C.

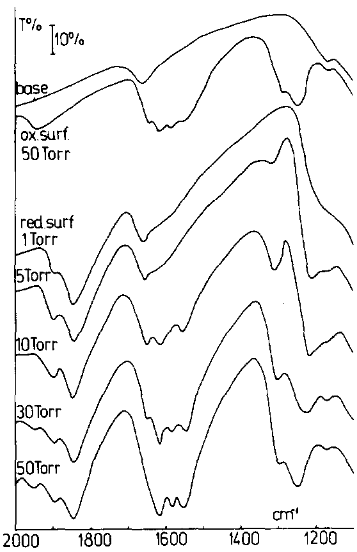

FIG. 3. Spectra observed at room temperature after dosing the reduced and oxidized sample with NO of various pressures at room temperature. The adsorption time was 30 min.

The intensities of the bands depended sensitively on the NO pressure. At the lowest pressure used (1–5 Torr) only the bands at 1900, 1850, and 1220 cm^{-1} could be detected. The intensities of the 1900 cm^{-1} and 1850 cm^{-1} bands reached saturation values at 10 Torr. The 1950 cm^{-1} band appeared from 30 Torr. Its intensity was always smaller than those of the above bands.

The bands between 1700 and 1500 cm^{-1} appeared only at higher pressure (the bands at 1620, 1590 and 1560 cm^{-1} were observed at 10 Torr); their intensities greatly increased with increase of pressure.

At higher adsorption temperatures the weak bands appeared in the spectra at significantly lower NO pressure. At 5 Torr NO the 1950 cm^{-1} band was detected first at 250°C. With further increase of the temperature its intensity slightly increased. In contrast, the 1900 cm^{-1} band showed a maximum at 200°C. The intensity of the 1850

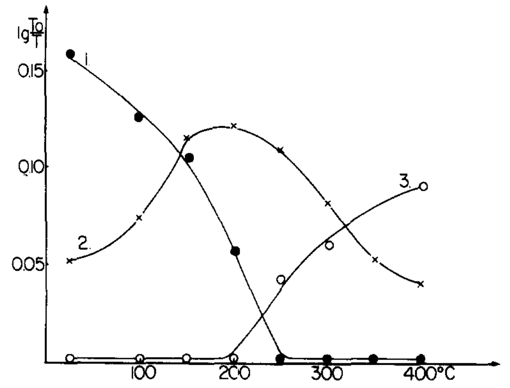

FIG. 4. The intensity of NO bands [(1) 1850 cm^{-1}; (2) 1900 cm^{-1}; (3) 1950 cm^{-1}] observed at room temperature after the adsorption of 5 Torr NO on reduced sample at different temperatures.

cm^{-1} band decreased monotonously with increasing temperature, and it did not appear above 200°C. Figure 4 shows the intensity changes of the above bands with the adsorption temperature.

In the subsequent experiments we investigated *the stability* of the bands observed after room temperature adsorption of NO. The gaseous NO was pumped off at room temperature for about 10 min.

The band at 1900 cm^{-1} intensified slightly from the beginning of the evacuation up to the tenth minute at 100–200°C; afterward it remained constant. At 300°C its intensity first increased, then decreased, and it disappeared quickly at 400°C. In contrast, the intensity of the 1850 cm^{-1} band decreased at all the temperatures. It was eliminated first at 300°C. The low intensity of the 1950 cm^{-1} band prevented detailed measurements. It can be stated, however, that it was somewhat more stable than the 1900 cm^{-1} band. The 1220 cm^{-1} band vanished very soon, even at 100°C. The other low-frequency bands were stable up to 200°C and disappeared quickly at 300°C. Figure 5 depicts the intensity-time curves obtained at different temperatures.

The spectra obtained after room temperature adsorption of NO *on oxidized surfaces* differed basically from those on reduced surfaces (Fig. 3). The bands at 1850 and 1900 cm^{-1} were missing and a weak 1950 cm^{-1} band appeared even at very low NO pressure. Its intensity slightly increased with the adsorption temperature up to 200°C, and it remained constant at 200–400°C. The intensities of the 1250, 1560, 1590, and 1620 cm^{-1} bands were almost the same as on reduced surfaces.

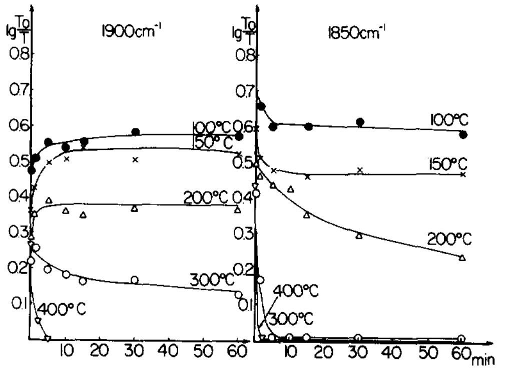

FIG. 5. The effect of evacuation and temperature on the intensities of the NO bands produced by the adsorption of 5 Torr NO at room temperature.

b. CO adsorption. The adsorption of CO at room temperature *on a reduced sample* caused bands at 2070–2060 and 2020 cm^{-1} (Fig. 6). Saturation values in their intensi-

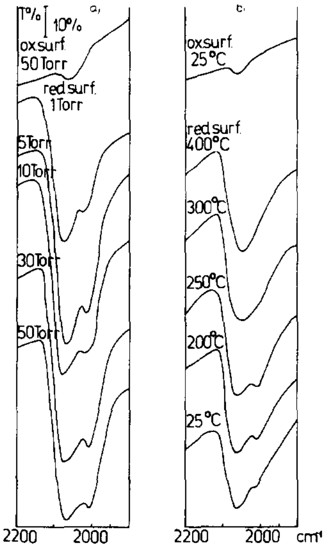

FIG. 6. Spectra observed at room temperature after dosing the reduced and oxidized sample (a) with CO of various pressures; and (b) with 5 Torr CO at different temperatures.

ties were reached even at a CO pressure of 10 Torr.

On increase of the adsorption temperature, the intensity of the high-frequency band increased up to 250°C (Fig. 6). At 300°C it was shifted to 2040 cm^{-1}. The intensity of the band at 2020 cm^{-1} increased with increasing temperature up to 150°C. Above 250°C, very likely due to the shift of the 2060 cm^{-1} band to 2040 cm^{-1}, the band at 2020 cm^{-1} could not be distinguished.

The stability of the adsorbed CO species was investigated in a similar way as for adsorbed NO. The adsorption temperature was 25°C. On heating up the sample during constant evacuation to 100°C, the intensities of both bands increased for a while, then slowly decreased in time. A great difference in the stabilities of the two bands can be seen clearly at 200°C, when the high-frequency band vanished in 10 min (Fig. 7). The complete disappearance of the 2020 cm^{-1} band occurred only at 400°C.

The spectra obtained *on oxidized surfaces* are shown in Fig. 6. At room temperature, only the band at 2070–2060 cm^{-1} appeared, with an intensity significantly smaller than on reduced surfaces. Variation of the CO pressure (1–50 Torr) hardly influenced its intensity. At higher adsorption temperatures, between 200 and 350°C, a great increase occurred in its intensity. It is noteworthy that above 300°C this band shifted to 2040 cm^{-1}. The 2020 cm^{-1} band was detected only at 250 and 300°C.

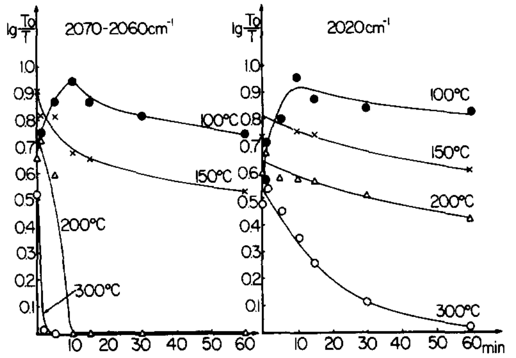

FIG. 7. The effect of evacuation and temperature on the intensities of the CO bands produced by the adsorption of 5 Torr CO at room temperature.

The frequencies of the bands due to adsorbed NO and CO are summarized in Table 2.

DISCUSSION

Adsorption Measurements

The adsorption of NO on Ir/Al_2O_3 was faster and stronger, and proceeded to a greater extent on reduced than on partially oxidized iridium. The NO is strongly bonded to the surface, as prolonged evacuation at 25–50°C resulted in only slight desorption. This is in agreement with the results of the infrared spectroscopic measurements. Dissociation of adsorbed NO was first detected at ~100°C by analyzing the gas phase during the adsorption and

TABLE 2

Infrared Bands Observed during the Adsorption of NO and CO

Adsorbate	Frequency (cm^{-1}) and structure							
CO	2070–2060 Ir–CO on Site A	2020 Ir–CO on Site B	1660 CO_3^{2-} on Al_2O_3	1450 CO_3^{2-} on Al_2O_3				
NO	1950 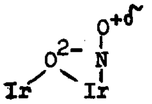	1900 $Ir–NO^{+\delta}$ on Site A	1850 $Ir–NO^{+\delta}$ on Site B	1620 NO_3^- on Al_2O_3	1590 NO_3^- on Al_2O_3	1560 NO_3^- on Al_2O_3	1310 NO_3^- on Al_2O_3	1220 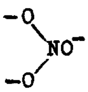 on Al_2O_3

thermal desorption measurements. It is very likely, however, that the dissociation of NO occurred to a small extent at lower temperatures, but the products of dissociation remained adsorbed on the surface, or, if they desorbed, their quantities were not large enough for them to be identified by mass-spectrometric analysis. According to ESCA studies, NO adsorbs molecularly at 170 K on an Ir single crystal with a (111) face; dissociation of adsorbed NO occurred above 323 K (*19*).

In the coadsorption of a NO + CO mixture at different temperatures, there was no significant increase of gas uptake which would automatically indicate promoted adsorption or formation of surface complex between NO and CO. This is in contrast to the findings with Pt/Al_2O_3 (*20*) and Pd/Al_2O_3 (*21*), where above 300°C the gas uptake from a NO + CO mixture was 1.5–2 times larger than the sum for the separately adsorbed gases. If we consider, however, that NO and CO adsorb on the same surface sites, even the measured extent of gas uptake, approaching the sum of the separately adsorbed gases, may be considered as an indication of some kind of promoted adsorption or surface complex formation.

Infrared Spectroscopic Measurement

Before attempting to interpret the spectra of adsorbed NO and CO, it is useful to consider *the types of bonding* occurring in nitrosyl and carbonyl complexes of transition metals and their *molecular orbital descriptions* (*22–26*). Two bonds, dative and π, exist between the metal ions and the ligands in these complexes. The σ bond results from an electron transfer from the filled σ orbital of the ligand to an unfilled d orbital on the metal. The π bond forms by back-donation of electrons from the d orbitals of the metal into the antibonding π^* orbital of the ligands. The formation of σ and π bonds leads to a cooperative strengthening of the metal–ligand bond. The back-donation, however, results in a slight weakening at the bond between the two atoms of the ligand.

As NO has an unpaired electron, the coordination mode of NO essentially depends on the relative energies of the π^* orbital of NO and of the metal d orbitals. In most cases transfer of an electron from the NO to the metal atom occurs, followed by coordination of the resulting NO^+. The M–N–O is linear in this case, and the electrons are localized to a greater extent on the nitrogen than on the oxygen atom. In the majority of NO complexes NO exists in this linear form, which gives vibrational frequencies in the range 1580–1980 cm^{-1}.

Coordination of NO as NO^- occurs much rarely. In this case the metal donates an electron toward the NO molecule. The resulting NO^- has a bent form, with an M–N–O angle of 120°. By gaining a more expressed π^* (antibonding) character, the NO bond loses energy, resulting in an increased N–O distance. Back-donation of an electron pair can also occur, however, from the π^* orbital of the NO^- to the metal d orbitals, and as a result the N–O bond has a more bonding character.

Previously it has been assumed that NO^- absorbs mainly at ca. 1200 cm^{-1}. Depending on the extent of the back-donation, however, the frequency of the ν(NO) vibration may increase up to 1700 cm^{-1}. Accordingly, Gans (*25*) suggested that when ν(N–O) is found in the region 1500–1700 cm^{-1}, the absorption band can be assigned to the structure NO^-.

Let us discuss first the *infrared spectra of adsorbed CO.*

Adsorption of CO on Ir/Al_2O_3 resulted in only two absorption bands, at 2070–2060 cm^{-1} and 2020 cm^{-1}, and we have not observed the very weak bands in the carbonyl region reported by Guerra and Schulman (*8*) on Ir/SiO_2. Our results, however, show a strong resemblance to those obtained by Howe (*9*) on highly dispersed Ir.

The intensity ratios of the bands varied considerably under different treatments, indicating that they belong to differently adsorbed species. The high-frequency band disappeared at lower temperatures than did the low-frequency band. The intensity changes in the two bands during outgassing suggest that part of the species giving the high-frequency band is transformed into the adsorbed form responsible for the low-frequency band.

In evaluating the structure of the adsorbed species it proved helpful to compare the vibrational frequencies for adsorbed NO and CO with those in metal complexes. Table 3 contains the N–O and carbonyl stretching frequencies for a number of iridium complexes. In these the carbonyl groups are present only in a terminal position. By comparison it seems acceptable to assign both bands to linearly bonded CO (M–CO). An alternative interpretation for the low-frequency band is to assign it to the bridged CO 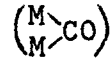. This assignment, however, seems unlikely in this case, as such structures normally have vibrational frequencies below 1900 cm^{-1}.

In contrast to the results on Rh/Al$_2$O$_3$, our infrared spectra provide no evidence for the presence of Ir(CO)$_2$ species, as such a structure would be expected to produce two infrared bands, with a constant intensity ratio corresponding to symmetric and asymmetric stretches of the carbonyl groups.

TABLE 3

NO and CO Vibrational Frequencies in Iridium Nitrosyls and Carbonyls (24, 26)

Compound	ν NO (CO) (cm^{-1})
[Ir(NO)(PPh$_3$)$_2$Cl$_3$]$^{1+}$	1945
[Ir(NO)(PPh$_3$)$_2$OH]$^{1+}$	1855
[Ir(NO)(PPh$_3$)$_2$(OEt)]$^{1+}$	1855
[Ir(NO)(PPh$_3$)$_2$Cl]$^{1+}$	1890
Ir(NO)(PPh$_3$)$_2$I$_2$	1576, 1564
[Ir(NO)(PPh$_3$)$_3$Cl]$^{1+}$	1710
Ir(NO){P(OPh)$_3$}$_3$	1740
C$_8$H$_{12}$Ir(NO)Cl$_3$	1685
[Ir(NO)(CO)(PPh$_3$)$_2$Cl]$^{1+}$	1690
[IrCl$_3$(CO)(PEt$_3$)$_2$]	2031
[IrCl$_3$(CO)(PBu$^n_3$)$_2$]	2034
[IrCl$_3$(CO)(PEt$_2$Ph)$_2$]	2070
[IrBr$_3$(CO)(PEt$_2$Ph)$_2$]	2056
[IrCl$_3$(CO)(AsEt$_3$)$_2$]	2060
[IrCl$_3$(CO)(AsEt$_2$Ph)$_2$]	2057

Our results rather suggest that there are two adsorptive sites on the surface, with different bonding properties, similar to what was proposed by Howe (9).

The high-frequency band can be assigned to CO adsorbed on metal atoms of larger iridium crystallites, in which the iridium atoms accessible to gas molecules have no interaction with the support (*Site A*). The low-frequency one can be attributed to CO adsorbed on an iridium atom of a cluster consisting of small numbers of iridium atoms influenced strongly by the support (*Site B*). This explanation is in harmony with the fact that the higher frequencies in the carbonyl complexes result from the reduced availability of d electrons due to the formation of Ir–Ir bonds.

The absence of Ir(CO)$_2$ species may suggest that, in spite of the high dispersity, our samples did not contain atomically dispersed iridium in sufficient concentration, or the bonding properties of isolated iridium atoms are different from those of rhodium. In this respect it is important to mention that this adsorbed species was missing when the Ir/Al$_2$O$_3$ sample was prepared by decarbonylation of Ir$_4$(CO)$_{12}$ on alumina, which resulted in a high dispersion of iridium (average metal crystallite size less than 2.0 nm) (9).

If we assume that corners and edges of small metal clusters are preferred sites for CO adsorption, the relative number of these places for *Site B* should be much greater than for *Site A*. In the case of rhodium, Yates (27) proposed that Rh exists as tiny "rafts" containing seven Rh atoms, with six atoms being edge atoms and behaving as if they are isolated.

The stability order of the two bands is in agreement with the model of carbonyl bonding which predicts that surface species characterized by high-frequency bands should be more weakly bound to the surface than structures characterized by low CO frequencies. The fact that the low-frequency band did not appear on a partially oxidized surface is understandable, as the iridium sites in high dispersity (*Site B*) are more easily oxidized.

Adsorption of NO on reduced surfaces at 25°C produced three adsorption bands, at 1850, 1900, and 1950 cm^{-1}. They differed considerably with respect to their occurrence and stability. The bands at 1900 and 1850 cm^{-1} appeared at room temperature and even on the application of a low pressure of NO. They were not identified on oxidized surfaces, however. The band at 1900 cm^{-1} was more stable against evacuation at elevated temperatures. The observation that the intensity of the 1900 cm^{-1} band increased during evacuation below 200°C, whereas that of the 1850 cm^{-1} band decreased, may indicate that the NO species responsible for the 1850 cm^{-1} band was transformed into the form causing the band at 1900 cm^{-1}.

Of these bands, only that at 1950 cm^{-1} was detected on oxidized surfaces. Taking into account its occurrence on such surfaces (discussed later), we ascribe this band to the adsorbed NO associated with partially oxidized Ir.

As the 1900 and 1850 cm^{-1} bands were not detected on oxidized surfaces, we may assume that these bands are associated with the NO adsorbed on reduced sites of Ir. There are several possibilities as regards assigning these bands. One possibility is that they represent the symmetric and asymmetric vibration of the structure 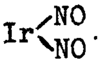 $\mathrm{Ir}{<}^{\mathrm{NO}}_{\mathrm{NO}}$. The different behaviors of the two bands, however, does not support the existence of this surface species.

A second possibility is to assign the high-frequency band to linearly bonded NO and the lower-frequency band to bridged NO. Whereas the latter form has been considered in many cases for adsorbed CO on supported metals, no importance has been given to this structure so far in the case of NO adsorption. Bridging nitrosyls in nitrosyl complexes exhibit lower stretching frequencies, below 1600 cm^{-1}, and thus this low-frequency band cannot be attributed to bridged NO. Very recently, however, using high-resolution electron energy loss spectroscopy, a band at 1411–1508 cm^{-1} due to adsorbed NO on Ru was assigned to the bridged form, and it was assumed that this bridged NO dissociates first (*28*).

The occurrence of the two bands may be interpreted by assuming that the reduced surface contains different adsorption sites, as proposed in the interpretation of the spectra of adsorbed CO.

Accordingly, we may attribute the more stable 1900 cm^{-1} band to the vibration of $NO^{+\delta}$ bonded on *Site A*, and the 1850 cm^{-1} band to the vibration of $NO^{+\delta}$ bonded on *Site B*. NO will adsorb on both sites by a partial transfer of electrons to the d orbitals of the iridium atoms

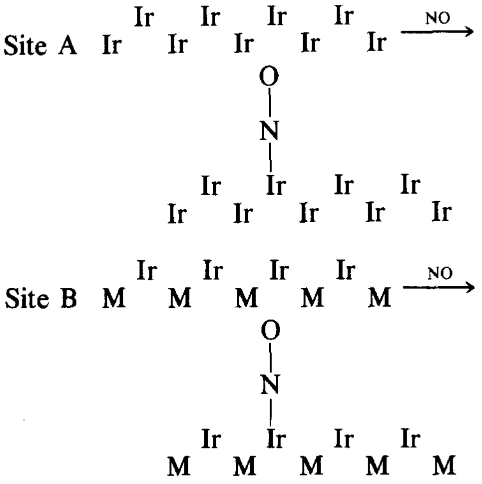

(1)

where M = metal ions of the support.

On increase of the temperature, the dissociation of adsorbed NO was first detected at 100°C. On the basis of the stabilities of the 1900 and 1850 cm^{-1} bands (Fig. 4), we proposed that the dissociation of NO will first occur on the more active centers, on *Site B*, and as a result these sites will be partially oxidized

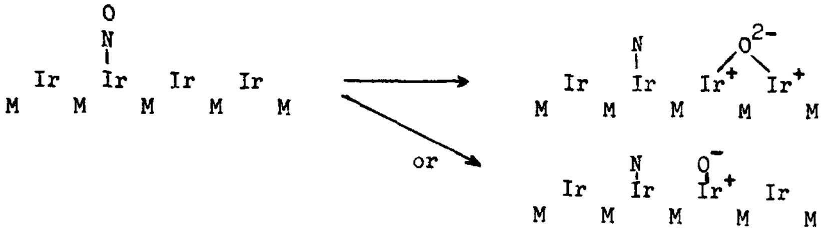

(2)

Consequently the surface concentration of this form of NO decreases. This is reflected in the gradual decrease in the intensity of the 1850 cm^{-1} band at higher adsorption temperatures, i.e., with the progress of the dissociation of NO, and in its complete elimination above 200°C (Fig. 4).

The subsequent adsorption of NO occurs mainly on this partially oxidized *Site B*, which again produces NO$^{+\delta}$ species;

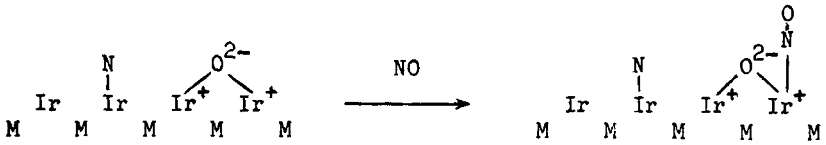

(3)

but due to the presence of O^{2-} ions fewer electrons of Ir are available for back-donation, and the N–O$^{+\delta}$ bond will be stronger and the vibrational frequency will be higher; the absorption band at 1950 cm^{-1} appears in the spectra. As the data in Fig. 4 show, its intensity grows with prolonged heating of the sample in NO or at elevated temperatures, in other words with the extent of NO dissociation. The observation that a weak band at 1950 cm^{-1} was detected at higher NO pressure at 25°C may indicate that limited dissociation of NO occurred on the most active particles (*Site B*) at this temperature, too.

At higher temperature the dissociation of adsorbed NO on *Site A* also occurs, similar to that proposed for *Site B*, and as a result NO can adsorb on the partially oxidized *Site A*, too. We obtained, however, only one band for NO adsorbed on oxidized surfaces; therefore, it is likely that the large perturbing effect of the oxygen ions on the Ir greatly overshadows the difference between the two adsorbing sites.

REFERENCES

1. Yang, A. C., and Garland, C. W., *J. Phys. Chem.* **61**, 1504 (1957).
2. Garland, C. W., Lord, R. C., and Troiano, P. F., *J. Phys. Chem.* **69**, 1188 (1965).
3. Yao, H. C., and Rotschild, W. G., *J. Chem. Phys.* **68**, 4774 (1978).
4. Arai, H., and Tominaga, H., *J. Catal.* **43**, 131 (1976).
5. Solymosi, F., and Sárkány, J., *Appl. Surface Sci.* **3**, 68 (1979).
6. Yates, J. T., Jr., Duncan T. M., Worley, S. D., and Vaughan, R. W., *J. Chem. Phys.* **70**, 1219 (1979).
7. Lynds, L., *Spectrochim. Acta* **20**, 1369 (1964).
8. Guerra, C. R., and Schulman, J. H., *Surface Sci.* **7**, 229 (1967).
9. Howe, R. F., *J. Catal.* **50**, 196 (1977).
10. Unland, M. L., *J. Catal.* **31**, 459 (1973).
11. Sinfelt, J. H., and Yates, D. J. C., *J. Catal.* **8**, 82 (1967).
12. Brooks, C. S., *J. Colloid Interface Sci.* **34**, 419 (1970).
13. Countour, J. P., and Pannetier, G., *Bull. Soc. Chim.* 3591 (1968).
14. Anderson, J. R., and Howe, R. F., *Nature (London)* **268**, 129 (1977).
15. Falconer, J. L., Wentrcek, P. R., and Wise, H., *J. Catal.* **45**, 248 (1976).

16. Vannice, M. A., *J. Catal.* **37**, 449 (1975).
17. Corro, G., and Gomez, R., *React. Kinet. Catal. Lett.* **9**, 325 (1978).
18. Weidenbach, G., and Fürst, H., *Chem. Technol.* **15**, 589 (1963).
19. Zhdan, P. A., Boreskov, G. K., Egelhoff, W. F., and Weinberg, W. H., Jr., *J. Catal.* **45**, 281 (1976).
20. Solymosi, F., Sárkány, J., and Schauer, A., *J. Catal.* **46**, 297 (1977).
21. Solymosi, F., and Sárkány, J., *in* "Proc. of the V. Ibero-American Symposium on Catalysis" (M. F. Portela, Ed.). Lisboa, 1976.
22. Eisenberg, R., and Meyer, C. D., *Accounts Chem. Res.* **8**, 26 (1975).
23. Blyholder, G., *J. Phys. Chem.* **68**, 2772 (1964).
24. Connelly, N. G., *Inorg. Chim. Acta Rev.* **6**, 47 (1972).
25. Gans, P., *J. Chem. Soc. Chem. Commun.* **8**, 144 (1965).
26. Cotton, F. A., and Wilkinson, G., "Advanced Inorganic Chemistry." Interscience, New York, 1972.
27. Yates, D. J. C., Conference on Catalyst Deactivation and Poisoning, May 24–28, 1978, Lawrence Berkeley Laboratory, Berkeley, Calif. 94720, Pub. 238.
28. Weinberg, W. H., Jr., private communication. Thomas, G. E., Thesis, California Institute of Technology, Pasadena, California, 1979.